Novel and Efficient Hw-Sw Developments in Millimeter Wave Antenna Measurement Facilities

Alfonso Muñoz-Acevedo[(1)], René Camblor Díaz[(2)], Yuri Álvarez López[(2)], Manuel Sierra-Castañer[(1)], Samuel Ver Hoeye[(2)], Fernando Las-Heras[(2)], José Luis Besada[(1)].
{alfonso ; m.sierra.castaner,besada }@gr.ssr.upm.es,
{rcamblor ; yalopez ; sverhoeye ; flasheras }@tsc.uniovi.es
[(1)] Grupo de Radiación, Dpto. de Señales, Sistemas y Radiocomunicaciones.
Universidad Politécnica de Madrid, Av. Complutense s/n, 28040 Madrid
[(2)] Área de Teoría de la Señal y Comunicaciones, Dpto. de Ingeniería Eléctrica.
Universidad de Oviedo. Edificio Polivalente, Módulo 8, Campus Universitario de Gijón, 33203 Gijón

***Abstract*- The aim of this communication is to show recent developments in the field of millimeter-wave antenna test ranges. Measurement facilities are complete systems used to acquire the radiated field by an antenna under test. When operating in millimeter waves, some common implementation principles become simply unaffordable. Manufacturing tolerances, structures computation times and available RF power offered by instrumentation become challenging aspects to cope with in millimeter waves. The developments shown in this paper focus on these issues.**

I. INTRODUCTION

Millimeter wavelength technologies are attracting, within the last years, the interest of scientists and engineers. Main reasons are the dense use of the electromagnetic spectrum and the development of new fields of application in the highest frequency band of RF technology.

The Terasense is a Spanish Government project, which aims to bring millimeter-wave technologies scientific knowledge on Spanish universities. Here, recent developments in the field of millimeter-wave antenna measurement are shown. A compact range and a planar acquisition system are separately studied as measurement facilities operating at millimetre and sub-millimeter wavelengths. In addition, *ad hoc* techniques, such as only-amplitude acquisitions and phase recovery algorithms are discussed.

II. COMPACT RANGE DESIGN

Compact ranges (CATRs) are well known antenna measurement facilities. Its principle of operation consists on generating far-field conditions so the radiation pattern of antennas under test are directly obtained. Different implementations reach far-field conditions; on one side, reflection-type compact ranges are most common options. On the other side, transmission-type compact ranges are based on collimator lenses, among which, holographic implementations have been proved to be effective in millimeter-wavelengths [5].

Our purpose here is to introduce a reflector-based compact range operating at 300 GHz. Constraints in the development of this system appear in the different subsequent stages of the process: design, construction and test. The proposed techniques aim to cope with the constraints at each sequential step.

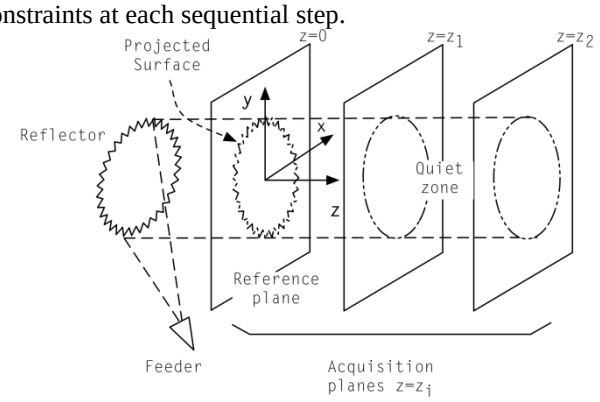

Fig. 1. Reflector-type compact range scheme

A. *Reflector design.*

Antenna measurements performance in compact ranges is directly related to the generated far-field distribution quality [2]. The region in which these conditions are generated is known as "quiet zone" and its specifications deal with amplitude as well as phase flatness. The quiet zone is located in the Fresnel region of the reflector which acts as a collimator and which reconfigures a spherical wavefront into a locally plane wave [3]. A scheme of the system is shown in Fig. 1.

Reflectors operating as quiet zone generators have particular characteristics, mainly related to edge treatment. Taking care of this, unwanted diffraction phenomena, which degrade the quiet zone performance, can be mitigated. Serrated edge [4] and rolled edge [6] reflectors are classical design options.

Moreover, an intrinsic feature of reflector operating as compact range collimators is its electrical size, which is mandatory to be large. The optimal design of large conformal edge reflectors is a challenging issue, which requires both results accuracy and non prohibitive computing times. Classical PO techniques are able to offer accurate results, with the drawback of taking unaffordable simulation times for large reflectors. On the other side, GO techniques are

several orders of magnitude faster, while not accurate enough for a complete design. Hybrid techniques including Planar Wave Spectrum formulations have been proposed [1] and are able to reach accurate results keeping reasonable computation times.

B. Millimeter wave instrumentation.

Main features in millimeter wave instrumentation are their output power and the available dynamic range. Typical figures at 300 GHz are -25dBm and 60 dB, respectively [8], being possible to increase the dynamic range by diminishing the IF filter bandwidth in the receptor and, thus, increasing the acquisition times. For single reflector ranges, a compromise must be reached between spherical wave attenuation between reflector and feeder, and quiet zone tapper due to the reflector illumination scheme.

C. Robustness to construction inaccuracies.

Construction inaccuracies in the reflector has, as a main consequence, high spatial frequency ripple in both amplitude and phase field distributions inside the quiet zone. At 300 GHz, usual surface accuracy $\lambda/100$ criterion becomes strict and requires a surface deviation below 10 micrometers. Thus, imperfections must be handled in the whole process in two different states. Firstly, the theoretical model [1] of analysis-design must be able to deal with these constraints and evaluate *a priori* the robustness to errors of a real reflector [7]. Secondly, correction techniques act *a posteriori*, being able to extract unwanted contributions taking into account both *a priori* information and real system calibration data. In this second stage, alignment and instrumentation errors can be also corrected if whole-system calibration schemes are developed.

III. Novel contributions to CATR reflector design

In this section, details are shown of the hybrid algorithm [1] already mentioned in the II.A. subsection. As presented in [9], the development of a computationally efficient algorithm has a major relevance if real design performance is needed, as in the case of a millimeter wave CATR.

The object of study, shown in Fig. 1. is divided into two well-defined radiation problems. On one side, typical F/D CATR reflectors in addition with low gain feeding schemes make possible the hypotheses that the collimator is in the far-field region of the feeder. Thus, GO ray tracing is enough to know the surface currents over the reflector.

The second stage of the algorithm consists on obtaining the plane waves vectorial spectral distribution, $\boldsymbol{A}(k_x, k_y)$, of the fed reflector [11]. This is obtained through integration of the reflected field over the projected surface, as shown in Eq. 1. It can be easily implemented with 2-dimensional FFTs over a M^2 points Nyquist-sampled electric field, as proposed in Eq. 2, for each field component.

$$\boldsymbol{A}(k_x, k_y) = \int_{-\infty}^{\infty}\int_{-\infty}^{\infty} \boldsymbol{E}(x, y, z=0)\cdot e^{jk_x\cdot x} e^{jk_y\cdot y} dk_x\, dk_y \tag{1}$$

The use of these numerical techniques under Nyquist criterion in addition with Analytical formulations [10] are able to obtain accurate results without information losses in the discretization process. The field is acquired at shifted z=constant planes by propagating the spectral information. Doing this, quiet zone acquisitions are obtained and CATR performance can be analyzed for particular reflectors, which is the algorithm's purpose and the basis of the reflector design process. A block scheme of the complete algorithm is shown in Fig. 2.

$$\begin{cases} A_{x,M}(k_x,k_y) = DFT^{-1}\{E_{x,M}(x,y,z=0)\} \\ A_{y,M}(k_x,k_y) = DFT^{-1}\{E_{y,M}(x,y,z=0)\} \\ A_{z,M}(k_x,k_y) = DFT^{-1}\{E_{z,M}(x,y,z=0)\} \end{cases} \tag{2}$$

$$\begin{cases} E_{x,M}(x,y,z) = DFT\left\{A_{x,M}(k_x,k_y)\cdot e^{-jk_z(k_x,k_y)z}\right\} \\ E_{y,M}(x,y,z) = DFT\left\{A_{y,M}(k_x,k_y)\cdot e^{-jk_z(k_x,k_y)z}\right\} \\ E_{z,M}(x,y,z) = DFT\left\{A_{y,M}(k_x,k_y)\cdot e^{-jk_z(k_x,k_y)z}\right\} \end{cases} \tag{3}$$

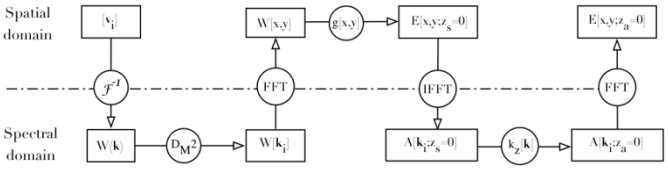

Fig. 2. Blocks scheme of the algorithm

IV. Planar Measurement Setup

A. Measurement setup description.

A planar measurement setup for sub-millimetre band antennas is proposed. This communication briefly describes the system, focusing on the near field-to-far field (NF-FF) transformation algorithms [12],[15], which have been widely tested in lower frequency bands [16],[17]. Most of sub-millimetre detectors, especially those that can provide better sensibility, are only suitable for amplitude measurements. These difficulties for phase measurements at sub-millimetre bands, makes the authors take phaseless measurements into consideration [14].

The proposed setup allows the acquisition of the 'x' and 'y' electric field components amplitude on several planes over the Antenna-Under-Test (AUT) (see Fig. 3). For this purpose, two horizontal sliders (for displacements along 'x' and 'y' axes) are required, jointly with a vertical slider in order to place the probe antenna on different planes.

B. Near field-to-far field transformation.

The proposed algorithm for NF-FF transformation using amplitude-only information is based on the use of an equivalent currents distribution to characterize the AUT, following the idea presented in [12],[15].

The integral equations relating the 'x' and 'y' electric field components with the 'x' and 'y' magnetic currents components are (4):

$$\begin{cases} E_x = -\dfrac{1}{4\pi}\displaystyle\int_{S'}\left(\frac{1+jk_0R}{R^3}\right)(z-z')e^{-jk_0R}M_y\,dS' \\ E_y = -\dfrac{1}{4\pi}\displaystyle\int_{S'}\left(\frac{1+jk_0R}{R^3}\right)(-z+z')e^{-jk_0R}M_x\,dS' \end{cases} \tag{4}$$

Or, in a more compact notation (5),

$$\begin{cases} E_y = G_1 \cdot M_x \\ E_x = G_2 \cdot M_y \end{cases} \quad (5)$$

Two decoupled linear equations are obtained, thus being able to be solved independently [13]. In the case of amplitude only data, two cost function are established, which relate the difference between the measured field amplitude, and the amplitude of the field radiated by the reconstructed equivalent magnetic currents (6):

$$\begin{cases} F_1 = \left\| \left| E_{y,meas} \right|^2 - \left| G_1 \cdot M_x \right|^2 \right\|^2 \\ F_2 = \left\| \left| E_{x,meas} \right|^2 - \left| G_2 \cdot M_y \right|^2 \right\|^2 \end{cases} \quad (6)$$

The cost function F_1 and F_2 are non-linear. In consequence, non-linear optimization techniques (Newton-Raphson [18], and Levenberg-Marquardt [18]) are applied to retrieve M_x and M_y from $E_{x,meas}$ and $E_{y,meas}$. Finally, from the reconstructed equivalent magnetic currents, the radiation pattern is calculated; it must be taken into account the angular margin validity due to the finite size of the planar acquisition surfaces.

C. Application example.

With the aim of testing the proposed methodology for NF-FF transformation using phaseless measurements, a rod antenna in the 600 GHz band has been simulated.

Dielectric rods have been studied since the middle of the last century [19]. They are travelling-wave antennas and are usually broadband.

As has been previously said, fabrication precision is a concern while working at 600 GHz and so is integration with other elements of the system, these two facts make dielectric rods especially suitable because they can be manufactured without great complexness and can be integrated with dielectric or metallic waveguides. As frequency increases dielectric waveguides become more interesting than metallic because no conductor losses are present.

Rod antennas can be found with rectangular shape tapered in E-plane, H-plane or in both. The one used here is a truncated cone 2.5λ high and it is fed by a metallic ring generated using a coplanar waveguide. This type of antenna has been implemented as a detector and can perform in array configuration [20]

The electric field radiated by the rod antenna is calculated on two planes placed at z_1 = 2 mm (4 λ) and z_2 = 4.5 mm (9 λ) over the rod antenna highest point. The acquisition planes' size (10 mm x 10 mm) is large enough to ensure that most of the radiated power is captured. Field samples are taken every 0.2 mm (0.4 λ) both in 'x' and 'y' axes. The reconstruction domain is a 2 mm x 2 mm plane, placed at the top of the rod antenna. Fig. 3 represents the planar field acquisition setup.

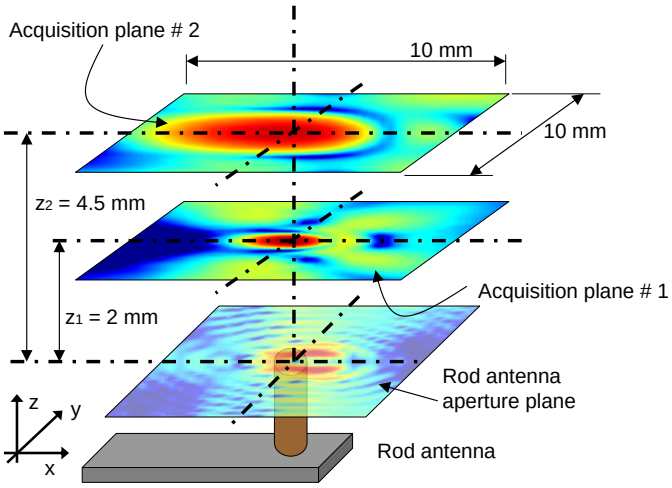

Fig. 3. Planar field acquisition setup and equivalent currents domain.

The equivalent magnetic currents (M_x, M_y) are reconstructed by minimizing cost functions F_1 and F_2 (6). Convergence is reached after 40 iterations of the Newton-Raphson method. The near field radiated by the reconstructed M_x, M_y is compared with the simulated ones (see Fig. 4).

In order to have a reference, the reconstructed M_x, M_y using amplitude-only information are compared with those ones calculated using amplitude and phase, as seen in Fig. 5.

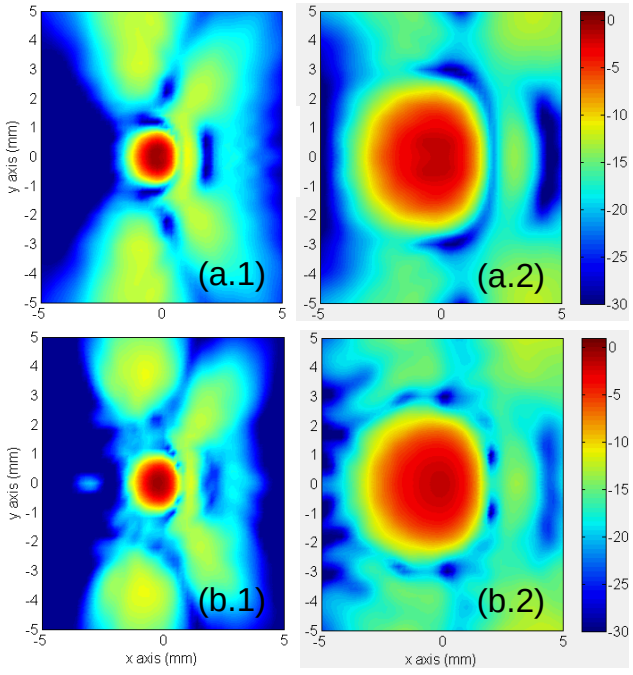

Fig. 4. Electric field (E_x component, normalized amplitude in dB) on the acquisition surfaces #1 and #2. (a.1) Simulated, z_1 = 2 mm (b.1) Reconstructed from M_y, z_1 = 2 mm (a.2) Simulated, z_2 = 4.5 mm (b.2) Reconstructed from M_y, z_2 = 4.5 mm

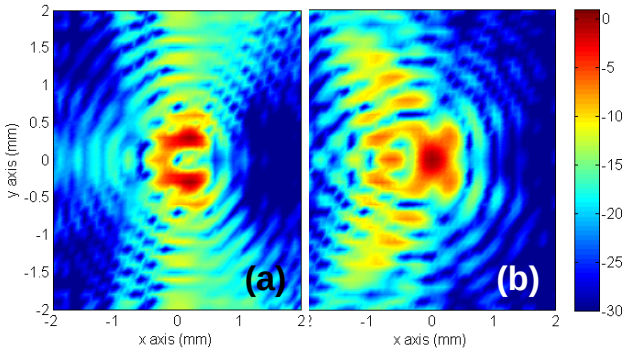

Fig. 5. Reconstructed equivalent magnetic currents (M_y component, normalized amplitude in dB). (a) From amplitude and phase near-field information. (b) From amplitude only near-field information.

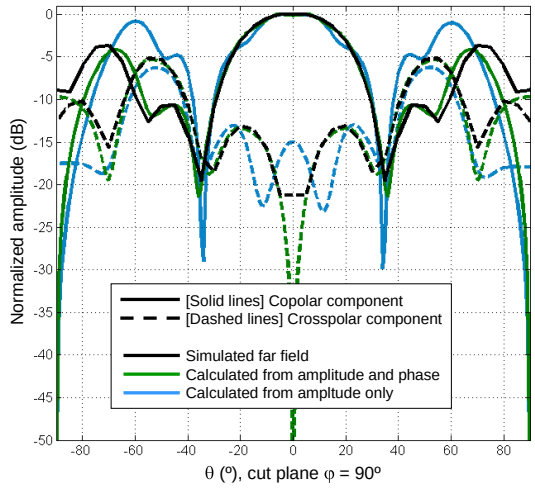

Fig. 6. Calculated radiation pattern using near-field amplitude and phase, and amplitude only information. Comparison with the simulated radiation pattern.

Last step is the far field pattern calculation from the reconstructed M_x, M_y. Fig. 6 compares the simulated far field with the pattern calculated using near field amplitude-only information, and amplitude and phase data. The agreement between radiation patterns in the main lobe region, both for copolar and crosspolar components, is reasonably good, especially taking into account the non high directive antenna under test that has been studied.

V. Conclusions

An algorithm for the design of compact ranges at millimetre and sub-millimeter frequencies based on hybrid GO-spectral formulations has been proposed and applied to the TERASENSE project.

In addition, a planar measurement setup for NF-FF transformation using phaseless measurements has been also presented. The reasonable accuracy of the results, even for non high directive antennas under test, confirms the applicability of those techniques at millimetre and submillimetre frequency bands.

Acknowledgements

This work has been supported by a Spanish Government FPI scholarship for Ph.D. students and both CROCANTE (TEC2008-06736-C03-01/TEC), INVEMTA (TEC2008-01638/TEC) and TERASENSE (CSD2008-00068) projects.

References

[1] A. Muñoz-Acevedo, M. Sierra-Castañer, J.L. Besada, "Analysis and Design of Serrated Compact Range Reflectors for mm-Wave Measurement Applications", in 2009 *Proc. Antenna Measurement Techniques Association Meeting*, Salt Lake City, 1-6 Nov. 2009.

[2] Parini, G., Philippakis, M.; "Use of Quiet Zone Prediction in the Design of Compact Antenna Test Ranges," *IEEE Trans. Antennas Propag.*, vol. 143, No.3, pp.193-199, Jun. 1996.

[3] R. L. Lewis and A. C. Newell, "An Efficient and Accurate Method for Calculating and Representing Power Density in the Near-zone of Microwave Antennas," *IEEE Trans. Antennas Propag.*, vol. AP-36, No. 6, Jun. 1988.

[4] E. B. Joy, R. E. Wilson, "Shaped Edge Serrations for Improved Compact Range Performance," in 1987 *Proc. Antenna Measurement Techniques Association Meeting*, Ottawa, 23-25 Sep. 1986.

[5] T. Koskinen, *Studies on an amplitude hologram as the collimator in a submillimeter-wave compact antenna test range*. Ph.D. dissertation, Helsinki University of Technology 2007.

[6] The-Hong Lee, W.D. Burnside, "Performance Trade-off Between Serrated Edge and Blended Rolled Edge Compact Range Reflectors," *IEEE Trans. Antennas Propag.*, vol. 44, Issue 1, pp.87-96, Jan. 1996.

[7] J. Ruze, "Antenna tolerance theory – a review," *Proceedings of the IEEE*, vol 54, Nº 4, April 1966.

[8] Agilent Millimeter-Wave Network Anallyzers technical overview. Available online: http://cp.literature.agilent.com/litweb/pdf/5989-7620EN.pdf

[9] A. Muñoz-Acevedo, M. Sierra-Castañer, "An Efficient Hybrid GO-PWS Algorithm to Analyze Conformal Serrated-Edge Reflectors for Millimeter-Wave Compact Range," *IEEE Trans. Antennas Propag.* [sent for review].

[10] Shung-Wu Lee, Mittra, R., "Fourier Transform of a Polygonal Shape Function and its Application in Electromagnetics," *IEEE Trans. Antennas Propag.*, vol.31, No. 1, pp. 99-103, Jan. 1983.

[11] P. A. Clemmow, *The Plane Wave Spectrum Representation of Electromagnetic Fields*, IEEE Press, New Jersey, Reissued Edition 1996.

[12] Y. Álvarez, F. Las-Heras, M. R. Pino, T. K. Sarkar, "An Improved Super-Resolution Source Reconstruction Method". *IEEE Transactions on Instrumentation and Measurement*, Vol. 58, Issue 11, pp. 3855-3866, November 2009.

[13] A. Taaghol, T. K. Sarkar, "Near-field to near/far-field transformation for arbitrary near-field geometry utilizing an equivalent magnetic current," *IEEE Transactions on Electromagnetic Compatibility*, Vol. 38, No. 3, August 1996, pp. 536-542.

[14] A. D. Hellicar, S. M. Hanham, G. Hislop, J. Du, "Terahertz Imaging with Antenna Coupled Detectors," Proc. on *3rd European Conference on Antennas and Propagation* (EuCAP'09). Berlin, 23-27 March 2009.

[15] F. Las-Heras, T. K. Sarkar, "A direct optimization approach for source reconstruction and NF-FF transformation using amplitude-only data," *IEEE Trans. on Ant. and Prop.*, Vol. 50, No. 4, Apr. 2002, pp. 500-510.

[16] R. G. Yaccarino, Y. Rahmat-Samii, "Phaseless bi-polar planar near-field measurements and diagnostics of array antennas," *IEEE Trans. on Antennas and Propagation*, Vol. 47, No. 3, March 1999, pp. 574-583.

[17] O. M. Bucci, G. D'Elia, G. Leone, R. Pierri, "Far-Field Pattern Determination from the Near-Field Amplitude on Two Surfaces," *IEEE Trans. on Ant. and Prop.*, Vol. 38, No. 9, Nov. 1990, pp. 1772-1779.

[18] *Numerical Recipes in C: the art of scientific computing.* Cambridge University Press 1988-1992. pp. 379-383 (Newton-Raphson) and pp. 681-688 (Levenberg-Marquardt). ISBN 0-521-43108-5.

[19] Leopold B. Felsen, "Radiation form Ring Sources in the Presence of a Semi-Infinite Cone," IRE Transactions on Antennas and Propagation, 1959.

[20] Stephen M. Hanham, Trevor S. Bird, Benjamin F. Johnston, Andrew D. Hellicar and Robert A. Minasian, "A 600 GHz Dielectric Rod Antenna," EuCAP 2009.